Bryozoan Skeletal Index (BSI): a measure of the degree of calcification in stenolaemate bryozoans

Patrick N. Wyse Jackson[1*], Marcus M. Key, Jr.[2] and Catherine M. Reid[3]

[1] Department of Geology, Trinity College, Dublin 2, Ireland
[*corresponding author: e-mail: wysjcknp@tcd.ie]
[2] Department of Earth Sciences, Dickinson College, Carlisle, Pennsylvania 17013-2896, USA
[e-mail: key@dickinson.edu]
[3] School of Earth and Environment, University of Canterbury, Private Bag 4800, Christchurch, New Zealand [e-mail: catherine.reid@canterbury.ac.nz]

ABSTRACT

The Upper Ordovician of the Cincinnati Arch region of the United States has yielded a highly diverse bryozoan fauna, and which provides an excellent data source for use in this study that proposes a novel measure of the degree of skeletal material in Palaeozoic stenolaemate bryozoans. This study is based on 16 trepostome species and one cystoporate species described from the Dillsboro Formation (Maysvillian to early Richmondian, Cincinnatian) of Indiana and in 20 species (15 trepostomes and five cystoporates) from the Lexington Limestone and Clays Ferry Formation (Middle to Upper Ordovician respectively) of Kentucky. The Bryozoan Skeletal Index (BSI) is derived from measurement of three characters readily obtainable from colonies: (1) maximum autozooecial apertural diameter at the zoarial surface or in shallow tangential section [MZD], (2) thickness of the zooecial wall between adjacent autozooecial apertures [ZWT], and (3) the exozone width [EW] in the formula:

$$BSI = ((EW*ZWT)/MZD)*100$$

This provides a measure of the relative proportion of skeleton to open space in the exozonal portion of the colony. The endozonal skeletal contribution to the overall colony skeletal budget is regarded as being minimal. In this study the differences observed in BSI between trepostome and cystoporate species in the Cincinnatian is significant, and ramose colonies show a higher BSI than encrusting zoaria in the same fauna.

INTRODUCTION

Bryozoans of the Class Stenolaemata are characterised by having autozooecial chambers that are broadly tubular in nature. They were significant members of the Palaeozoic faunas appearing in the Ordovician when there was a rapid diversification into six orders (Ernst 2019, fig. 1). While the majority of these groups disappeared at the Permo-Triassic boundary, some trepostomes, cystoporates, and one cryptostome survived in reduced diversity into the Triassic (Boardman 1984, Powers and Pachut 2008), while the cyclostomes took advantage of vacated niches and diversified rapidly in the Mesozoic before they declined and members of the Class Gymnolaemata overtook them in terms of diversity (Ernst 2019).

Within the stenolaemates classes, the trepostomes together with the esthonioporids developed the greatest degree of calcification in their colonies, followed by the cystoporates, cryptostomes, and cyclostomes, whereas the fenestrates were least calcified. All of these orders with the exception of the cyclostomes have recently been assembled together into the subclass Palaeostomata (Ma *et al.*, 2014). As Taylor *et al.* (2015) note, these are skeletally rather different from the cyclostomes which have frontal walls that are calcified.

Key (1990) developed a morphometric approach to quantifying the amount of skeleton in ramose trepostomes colonies using ZWT and MZD compared between the endozone and exozone. That study showed that the endozonal skeletal contribution to the overall colony skeletal budget is minimal. This study takes a more generic approach that is applicable to ramose, encrusting, frondose, and massive stenolaemates of all classes. Herein we establish the Bryozoan Skeletal Index (BSI), a novel measure of the degree of exozonal skeletal material in stenolaemate bryozoans.

This current study is one of a continuum of papers by the authors on various aspects of Cincinnatian bryozoans which together with other recent studies have added to our understanding of the inter-relationship of these bryozoans with endoskeletozoans (Erickson and Bouchard 2003; Wyse Jackson *et al.* 2014; Wyse Jackson and Key 2019) and epizoozoans (Baird *et al.* 1989; Wyse Jackson *et al.* 2014), and the character of their growth, branching and reasons for colony fragmentation (Key *et al.* 2016) as well as their palaeoecological setting (Buttler and Wilson 2018). The Ordovician was a time of calcite seas and bryozoans thrived during the Cincinnatian, so much so that Taylor and Kuklinski (2011) asked whether trepostomes had become hypercalcified at this time. Bryozoans that in life encrusted on living aragonitic molluscs have yielded much information about the host shells that rapidly dissolved in these calcitic seas and their early stage epibionts and endobionts which are known only from the bryoimmurations (Wilson *et al.* 2019). This recent research adds to the wealth of information on Cincinnatian bryozoans published since the late nineteenth century (see Key *et al.* 2016, p. 400 for summary).

Size of bryozoan colonies and skeletal materials have been the focus of various studies that have taken specific avenues. Key (1990, 1991) examined parameters that influenced skeletal size in trepostome bryozoans, Cheetham (1986) showed that Cenozoic cheilostomes developed the ability to thicken branches, and Cheetham and Hayek (1983) discussed the ecological implications of being able to produce robust and erect bryozoan colonies. Key *et al.* (2001) showed how a Permian trepostome with a notably wide exozone achieved this size not by secreting more skeleton but by inserting exilazooecia within maculae. Cuffey and Fine (2005, 2006) reconstructed the largest trepostomes colonies from fragments.

Thus, understanding the architecture and abundance of skeleton in stenolaemates is important for a number of reasons, and the BSI proposed here which is straight forward to derive, allows for rapid comparison between taxa of different stenolaemates. Amongst a number of aspects, the BSI can be utilised as a measure of strength of zoaria and ability to withstand infestation by endoskeletozoans. If a higher BSI allows upward vertical growth with the ramose zoarial habit, then those colonies have access to resources in the water column that are not available to encrusting colonies confined to the substrate (Jackson 1979). The robustness of the BSI is tested here utilising a suite of Ordovician trepostome and cystoporate bryozoans.

MATERIALS

The Cincinnatian of the Upper Ordovician of the United States has yielded a highly diverse bryozoan fauna with a range of morphological forms (Fig. 1) that has been extensively reported since the 1850s, and thus provides an excellent database for use in this study that proposes a novel measure of the degree of skeletal material in Palaeozoic stenolaemate bryozoans.

This study is based on bryozoans described from the Lexington Limestone and Clays Ferry Formation (Middle [Sandbian] to Upper Ordovician [Sandbian-Katian] respectively) of Kentucky (Karklins 1984) and the Dillsboro Formation (Maysvillian to early

Richmondian [Katian], Cincinnatian) of south-eastern Indiana (Brown and Daly 1985). Karklins (1984) reported on 36 species in 22 genera (16 trepostomes and six cystoporates) while Brown and Daly (1985) provided detailed taxonomic descriptions for 53 species in 18 genera of which 17 belonged to the Order Trepostomata and one to the Order Cystoporata. These two taxonomic studies provide a suite of data (a total of 37 species, Table 1) that allow for initial testing of the robustness of the BSI formula prior to it being utilised in further and larger studies (see below).

METHODS

The Bryozoan Skeletal Index (BSI) is derived from three measures: (1) maximum autozooecial apertural diameter at the zoarial surface or in shallow tangential

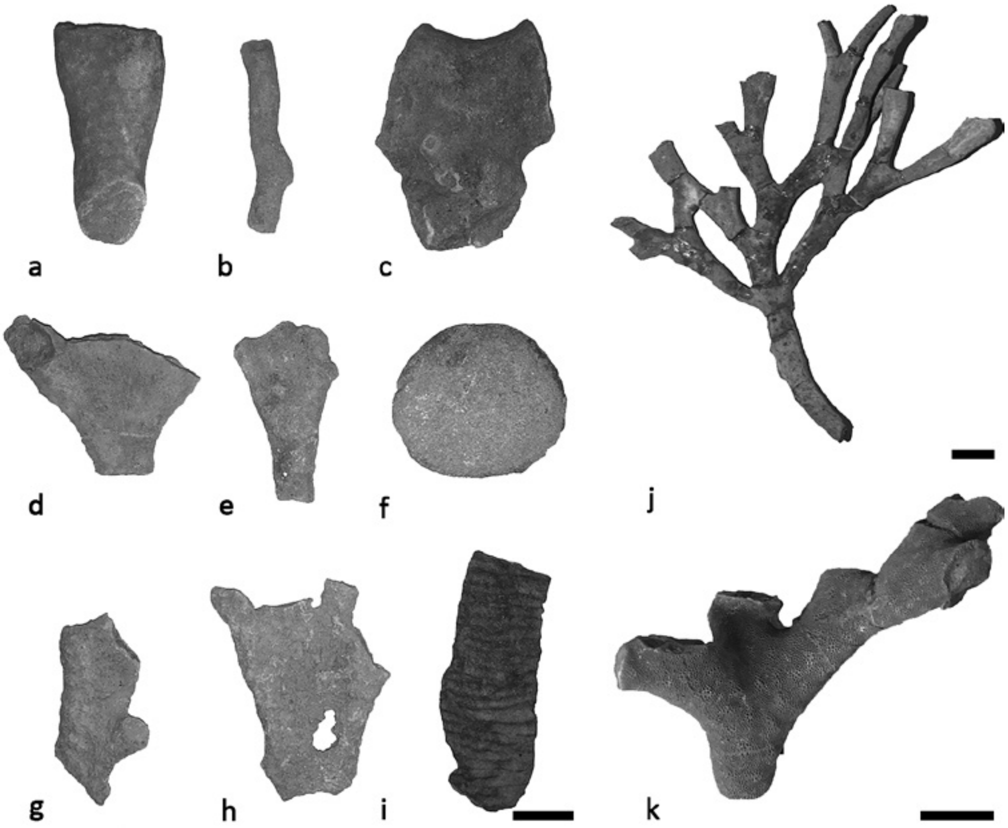

Figure 1. Cincinnatian Bryozoa (a-c) ramose trepostomes; (d-e) foliose trepostomes; (f) domed trepostome; (g-h) foliose cystoporate (*Constellaria* sp.); (i) bifoliate cryptostome (*Escharopora hilli*) from the Lexington Limestone, Kentucky, USA, (a-e, g-i) from Stafford, Kentucky, road-cut on west side highway 150 (37°34.97N 84°42.68W); (f) from Danville, Kentucky, junction 150 and bypass, Danville sign (37°38.73N 84°46.59W), Geological Museum, Trinity College Dublin. (j) re-assembled ramose trepostome *Hallopora andrewsi* (Nicholson, 1874) from Southgate Member, Kope Formation, Western corner of the intersection of Rt. 9 (AA Highway) and Kentucky Rt. 709 (US 27-AA Highway Connector Rd.) adjacent to Alexandria, KY; on slope leading down to Rt. 709; 38.988753°N, 84.396203°W, CMC IP72749. (k) ramose trepostome *Hallopora subplana* (Ulrich, 1882), Mount Hope Member, Fairview Formation, Covington, Kentucky, USNM 40364. (j, from Key et al., 2016, fig. 1.5). Scale bars = 10mm.

Table 1. Bryozoan Skeletal Index (BSI) index for Cincinnatian (Katian) stenolaemate bryozoans. Abbreviations: MZD = mean autozooecial apertural diameter (in mm); EW = mean exozone width (mm); ZWT = mean thickness of the zooecial wall between adjacent autozooecial apertures at zoarial surface or in shallow tangential section (in mm); B & D = Brown and Daly.

Order	Taxon	Zoarial form	MZD	EW	ZWT	BSI	Source	Lithological unit (Stage)
Trepostomata	*Orbignyella lamellosa*	encrusting	0.216	2.976	0.017	23	B & D, 1985	Dillsboro (Katian)
Trepostomata	*Mesotrypa patella*	encrusting	0.216	1.810	0.010	8	B & D, 1985	Dillsboro (Katian)
Trepostomata	*Leptotrypa minima*	encrusting	0.217	2.146	0.010	10	B & D, 1985	Dillsboro (Katian)
Trepostomata	*Monticulipora mammulata*	massive	0.210	2.488	0.015	18	B & D, 1985	Dillsboro (Katian)
Trepostomata	*Peronopora vera*	bifoliate	0.197	2.238	0.049	56	B & D, 1985	Dillsboro (Katian)
Trepostomata	*Amplexopora septosa*	ramose	0.231	1.333	0.038	22	B & D, 1985	Dillsboro (Katian)
Trepostomata	*Parvohallopora ramosa*	ramose	0.220	0.950	0.080	35	B & D, 1985	Dillsboro (Katian)
Trepostomata	*Batostomella gracilis*	ramose	0.154	1.463	0.075	71	B & D, 1985	Dillsboro (Katian)
Trepostomata	*Batostoma varians*	ramose	0.279	2.585	0.098	90	B & D, 1985	Dillsboro (Katian)
Trepostomata	*Cyphotrypa madisonensis*	ramose	0.287	1.317	0.015	7	B & D, 1985	Dillsboro (Katian)
Trepostomata	*Dekayia catenulata*	ramose	0.199	1.503	0.018	14	B & D, 1985	Dillsboro (Katian)
Trepostomata	*Nicholsonella vaupeli*	ramose	0.271	0.976	0.065	23	B & D, 1985	Dillsboro (Katian)
Trepostomata	*Rhombotrypa quadrata*	ramose	0.250	1.050	0.033	14	B & D, 1985	Dillsboro (Katian)
Trepostomata	*Stigmatella interporosa*	ramose-frondescent	0.213	0.650	0.020	6	B & D, 1985	Dillsboro (Katian)
Trepostomata	*Heterotrypa subfrondosa*	frondescent	0.204	1.303	0.029	19	B & D, 1985	Dillsboro (Katian)
Trepostomata	*Homotrypa flabellaris*	frondescent	0.163	1.415	0.047	41	B & D, 1985	Dillsboro (Katian)
Cystoporata	*Constellaria polystomella*	frondescent	0.133	1.317	0.062	61	B & D, 1985	Dillsboro (Katian)
Trepostomata	*Mesotrypa angularis*	domal	0.2450	5.9000	0.0360	87	Karklins, 1994	Lexington Ls. (Sandbian)
Trepostomata	*Cyphotrypa acervulosa*	globular	0.2687	2.5000	0.0110	10	Karklins, 1994	Lexington Ls. (Sandbian)
Trepostomata	*Prasopora falesi*	hemispherical	0.2513	3.0000	0.0173	21	Karklins, 1994	Lexington Ls./Clays Ferry Fm. (Sandbian-Katian)
Trepostomata	*Peronopora vera*	bifoliate	0.1860	1.6180	0.0583	51	Karklins, 1994	Lexington Ls./Clays Ferry Fm. (Sandbian-Katian)
Trepostomata	*Homotrypella granulifera*	ramose	0.1380	1.3110	0.0880	84	Karklins, 1994	Lexington Ls. (Sandbian)
Trepostomata	*Parvohallopora nodulosa*	ramose	0.2296	0.7529	0.0718	24	Karklins, 1994	Lexington Ls./Clays Ferry Fm. (Sandbian-Katian)
Trepostomata	*Eridotrypa mutabilis*	ramose	0.1888	0.9370	0.0961	48	Karklins, 1994	Lexington Ls./Clays Ferry Fm. (Sandbian-Katian)
Trepostomata	*Tarphophragma multitabulata*	ramose	0.2552	0.7188	0.0470	13	Karklins, 1994	Lexington Ls. (Sandbian)
Trepostomata	*Heterotrypa foliacea*	ramose	0.1950	1.2200	0.0496	31	Karklins, 1994	Lexington Ls./Clays Ferry Fm. (Sandbian-Katian)
Trepostomata	*Homotrypa cressmani*	ramose	0.1260	1.0200	0.0840	68	Karklins, 1994	Lexington Ls./Clays Ferry Fm. (Sandbian-Katian)
Trepostomata	*Atactoporella newportensis*	ramose	0.1500	0.2125	0.0580	8	Karklins, 1994	Lexington Ls./Clays Ferry Fm. (Sandbian-Katian)
Trepostomata	*Amplexopora* aff. *winchelli*	ramose	0.2078	1.7000	0.0367	30	Karklins, 1994	Lexington Ls. (Sandbian)
Trepostomata	*Balticopora tenuimurale*	ramose	0.2665	1.3000	0.0429	21	Karklins, 1994	Lexington Ls./Clays Ferry Fm. (Sandbian-Katian)
Trepostomata	*Dekayia epetrima*	ramose	0.2120	3.0000	0.0240	34	Karklins, 1994	Lexington Ls. (Sandbian)
Trepostomata	*Stigmatella multispinosa*	subconical	0.2095	0.8333	0.0140	6	Karklins, 1994	Lexington Ls. (Sandbian)
Cystoporata	*Ceramoporella distincta*	encrusting	0.2915	0.3963	0.0260	4	Karklins, 1994	Lexington Ls. (Sandbian)
Cystoporata	*Crepipora venusta*	encrusting	0.2530	0.5800	0.0452	10	Karklins, 1994	Lexington Ls./Clays Ferry Fm. (Sandbian-Katian)
Cystoporata	*Acanthoceramoporella valliensis*	globular	0.2300	1.0500	0.0288	13	Karklins, 1994	Lexington Ls. (Sandbian)
Cystoporata	*Ceramophylla alternatum*	ramose?	0.2133	0.5000	0.0940	22	Karklins, 1994	Lexington Ls./Clays Ferry Fm. (Sandbian-Katian)
Cystoporata	*Constellaria teres*	ramose	0.1198	1.8333	0.0175	27	Karklins, 1994	Lexington Ls./Clays Ferry Fm. (Sandbian-Katian)

section [MZD], (2) thickness of the zooecial wall between adjacent autozooecial apertures [ZWT], and (3) the width of the exozone [EW] all measured in mm (Fig. 2). Parameter 1 is a measure of the open space in the exozonal region, whereas parameters 2 and 3 are features of largely solid skeletal material.

$$BSI = ((EW*ZWT)/MZD) *100$$

The resultant computation is multiplied by 100 so as to give a whole number.

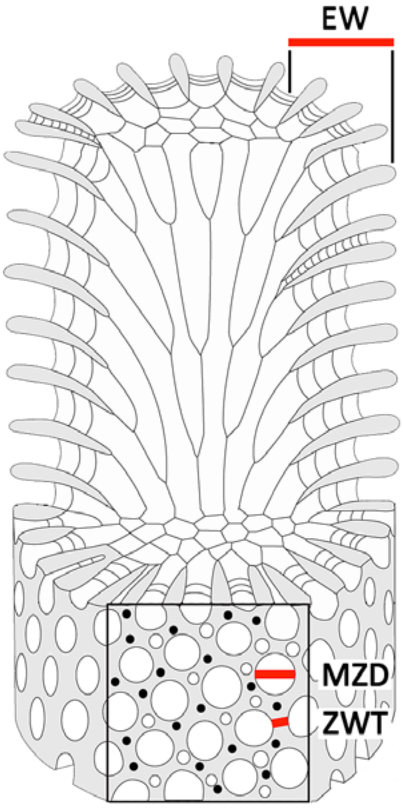

Figure 2. Morphological characters used to compute the Bryozoan Skeletal Index (BSI) (modified from Ernst and Carrera 2012, after Boardman 1984). Abbreviations: MZD: maximum autozooecial apertural diameter at the zoarial surface or in shallow tangential section; ZWT: thickness of the zooecial wall between adjacent autozooecial apertures; EW: thickness of the exozone.

In many of these stenolaemate bryozoans, colonies are made up of an innermost endozone with thinner walls surrounded (or overlain as in the case of encrusting zoaria) by an outer exozonal rim of thickened skeleton. In contrast to these, in some globular and dome-shaped trepostomes such as *Diplotrypa* the endozone comprises a thin, recumbent layer at the base and exozonal walls generally are thin. In any one taxon, the thickness of the exozone is given to remain proportionally constant to that of the colony diameter.

The three parameters above were chosen to provide a measure of the relative proportion of skeleton to open space in the exozonal portion of the colony. No endozone parameters (e.g., endozone diameter, branch diameter, axial ratio, etc.) were included as the zooecial walls in the endozone of trepostomes are significantly thinner (i.e., less skeletalised) than those in the exozone (Key 1990, fig. 3). The endozonal skeletal contribution to the overall colony skeletal budget is considered to be minimal. Axial Ratio (Boardman 1960, p. 21) may be calculated from ramose colonies but not from encrusting forms. Additionally, adoption of this measure is problematic as it cannot be computed in zoaria that have been subjected to post-depositional crushing, where the endozone collapses but the exozonal width is unaffected (Key *et al.* 2016, fig. 2.6). This would reduce the number of specimens collected from many faunas that otherwise could be added to the data suite.

Details of these three parameters are usually reported in taxonomic literature as they are easy to acquire. For this study, data was taken from only one species per genus reported in Karklins (1984) and Brown and Daly (1985); that for which data on each of the relevant parameters was selected, and where several taxa presented this complete data, the type species if described was favoured. Otherwise, then the species for which the greatest number of morphometric measurements was reported was selected; an abundant species is most likely to yield robust morphometric data on the three parameters than from a rarer species. Karklins (1984) tabulated data for primary types separately to that for hypotypes (specimens not part of the original type suite), and in this case we selected the morphometric data derived from the largest number of measurements, which resulted in not necessarily selecting data from primary holotypes or paratypes. Where not all relevant character values for BSI computation were reported in the published data tables, these were obtained from the figured plates where scale bars scales were provided, or by collating data from a suite of specimens reported in the papers.

During data gathering for this study, additional information was compiled on lithostratigraphy (from the original publication), chronostratigraphic stage (Haq 2007), geological age (Cohen *et al.* 2013), and palaeolatitude (van Hinsbergen *et al.* 2015). This will allow for the determination of trends in the BSI through space and time in a further on-going study to be published elsewhere.

It may be considered that the BSI would be more accurate if it was based on three-dimensional characters such as the volume of space occupied by autozooecial, mesozooecial or exilazooecial chambers, as well as the volume of exozonal and endozonal walls, the portions of acanthostyles that extend beyond the surficial margins of autozooecial walls, and any intrazooecial features such as widely spaced monilae in the exozone, skeletal diaphragms, hemiphragms, and cystiphragms (Boardman 2001; Boardman and Buttler 2005). The effect of these features on the BSI values could be computed by adding those additional characters composed of solid skeleton such as acanthostyles to the left-hand side of the equation alongside EW and ZWT and those of the open spaced features (exilazooecia and mesozooecia) to the right-hand side in combination with MZD. Similarly, the effect of maculae on skeletal volume could be tested. Some monticulate maculae may be skeletal rich (Fig. 1g-h), whereas others that contain numerous exilazooecia and which are flush with the zoarial surface probably add little to the skeletal budget of zoaria (Fig. 3g). For this paper, that establishes the BSI, it was felt prudent to derive a simple equation and to test its effectiveness. The equation as proposed nonetheless allows for additional extrazooidal characters such as those outlined above, to be added in the future as desired.

The overall geometry of autozooecial chambers varies from taxon to taxon, with many chambers being cone-shaped and others more parallel sided and so cylindrical in form. Quantification of three-dimensional volumes would be complex, time-consuming and prone to high levels of measurement error. Many trepostome taxa possess autozooecial and mesozooecial chambers that contain intrazooecial divisions such as diaphragms (e.g., *Hallopora*) and cystiphragms (e.g., *Prasopora*), and cystoporate genera typically possess vesicular tissue between adjacent autozooecial chambers. For the purpose of this study we consider that the overall volume contributed by these intra- and extrazooecial elements to be negligible compared to the volume of skeleton contained in the autozooecial walls throughout the depth of the exozone. Boardman (2001) noted that structural diaphragms can be extensively developed in some trepostome taxa, although these are very narrow and so contribute low levels of skeleton overall. If necessary a factor could be added to the BSI calculation to account for their development in some taxa. Users applying the BSI should also note that proximal portions of colonies may have thickened walls and endozones compared to younger distal regions, and measuring in areas of macular development may modify the resultant BSI values. Additionally, while the monographs utilised in this study are detailed, information on all the intra and extra-zooecial parameters above is rarely provided for every taxon.

Supporting greater accuracy to BSI calculations would be to consider the nature of the skeletal ultrastructure, which as Taylor *et al.* (2015) reviewed is somewhat varied within the members of the Palaeostomata and more so between them and the other stenolaemate order, the cyclostomes. In this study we have not attempted to quantify palaeostomate ultrastructure, and it has not been used as a BSI parameter.

RESULTS

The BSI of these 37 Cincinnatian stenolaemates ranges from values of 4 to 90 (mean = 30.5; standard deviation = 24.2, Table 1). The lowest BSI in an encrusting species was 4 in the cystoporate *Ceramoporella distincta* from the Lexington Limestone whereas the highest was 23 in the trepostome *Orbignyella lamellosa* (Fig. 3a-b) from the Dillsboro Formation. In ramose trepostomes the lowest BSI was 6 in *Stigmatella interporosa* (Fig. 3i-k) and the highest was 90 in *Batostoma varians* (Fig. 3e-f) both from the Dillsboro. One species *Peronopora vera* which formed bifoliate colonies was common to both of the original studies investigated with the BSI 51 in the Lexington Limestone/Clays Ferry material and slightly higher at 56 in the Dillsboro Formation.

Encrusting bryozoans in the stratigraphically older successions of Kentucky recorded BSIs of 4–10 (n = 2, mean = 7.0, standard deviation = 4.9) as compared to those from the younger Dillsboro Formation of Indiana with BSI of 8–23 (n=3,

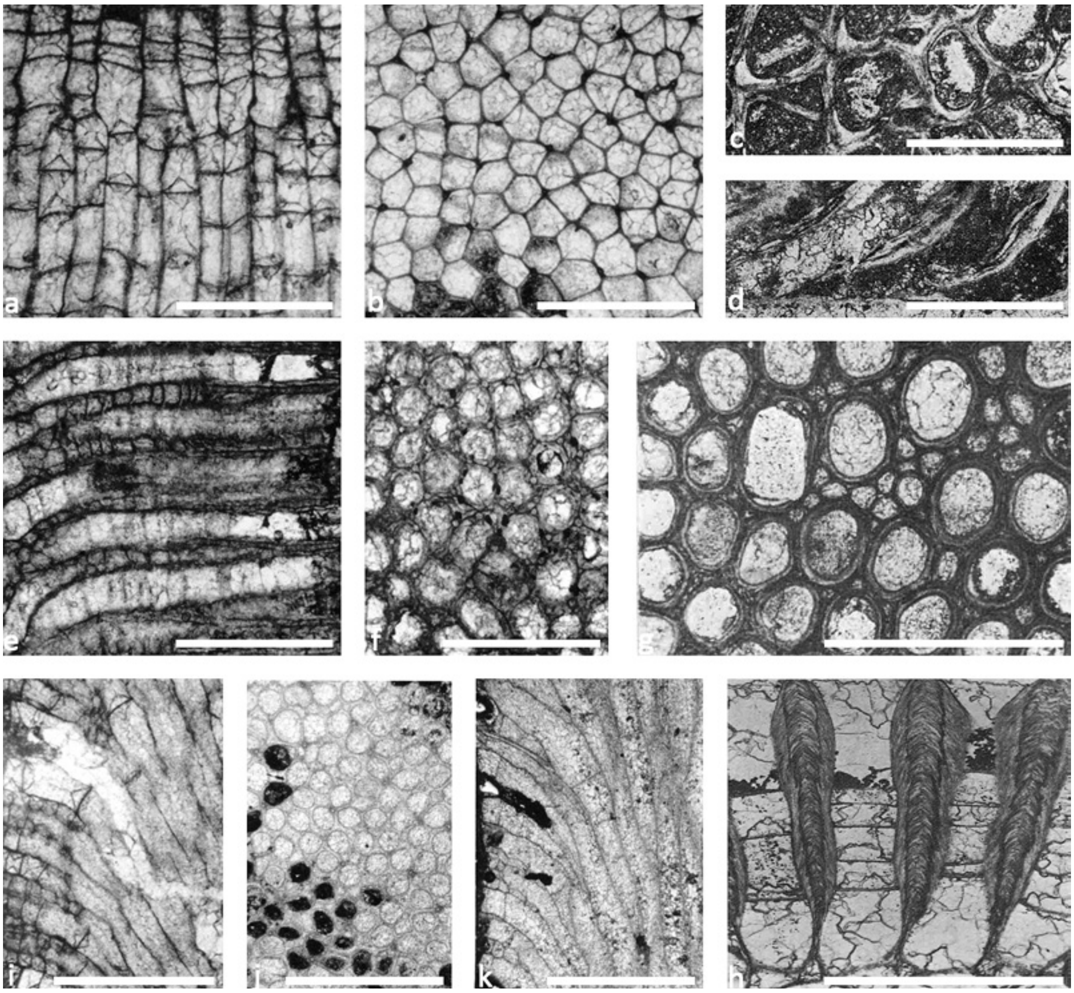

Figure 3. (a-d) Encrusting bryozoans; (e-k) Ramose bryozoans. (a-b) *Orbignyella lamellosa* (Ulrich, 1890); (c-d) *Crepipora venusta* (Ulrich, 1878); (e-f) *Batostoma varians* (James, 1878), (g-h) *Parvohallopora ramosa* (d'Orbigny, 1850); (i-k) *Stigmatella interporosa* Ulrich and Bassler, 1904. [c-d, g-h from Karklins, 1984; a-b, e-f, i-k from Brown and Daly, 1985). Scale bars = 0.5mm (c, d, h), 1mm (a, b, e-f, i-k).

mean= 13.9, standard deviation=8.3). Ramose bryozoans in the two units exhibited nearly identical BSI ranges: 8–84 (n = 13, mean = 31.9, standard deviation=22.6) as against 6–90 (n = 14, mean = 31.3, standard deviation = 29.8). Domed, globular, massive or hemispherical zoaria from the older unit ranged in value from 10 to 87 (n = 4, mean = 32.7, standard deviation=36.3) and frondose colonies in the Dillsboro had a BSI range of 19–61 (n = 3, mean = 40.2, standard deviation = 21.5).

The cystoporates (n = 6), regardless of zoarial habit or stratigraphic range, generally had lower BSI values (range = 4-61, mean = 22.9, standard deviation=18.8) than the trepostomes (n = 31, range = 6-90, mean = 32.0, standard deviation = 24.9), but it they were not significantly different (t-Test, P = 0.371, Fig. 4a, 5a). Adding data from cystoporates in other faunas might demonstrate that they exhibit a similarly broad range as do the trepostomes measured in this study. A wider assessment in terms of taxa in space and time will be undertaken in a future study.

The encrusting taxa (n = 5) (Fig. 3a-d), regardless of stratigraphic age and taxonomy, generally showed a lower BSI with a range of 4–23 (mean = 11.1; standard deviation = 6.6, Table 1), and conversely

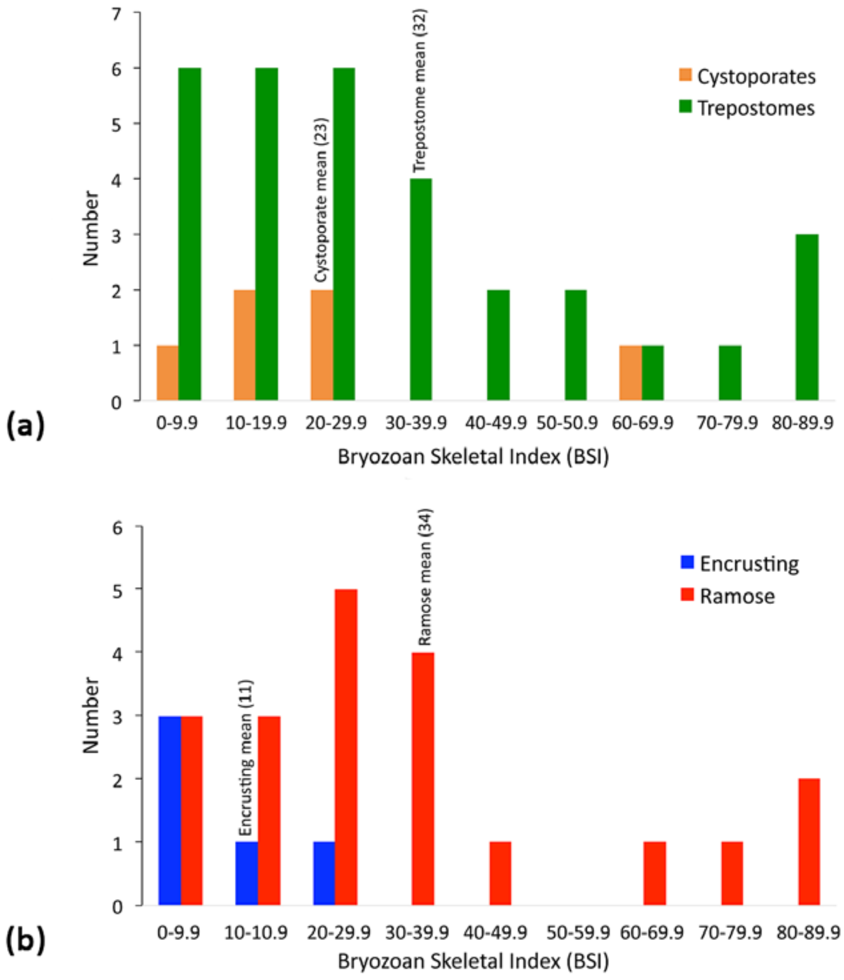

Figure 4. Frequency histograms show the numbers of taxa within groupings of BSI for (a) cystoporates and trepostomes and (b) encrusting and ramose colonies.

ramose zoaria (n = 20) (Fig. 3e-j) yielded higher BSI values in the range 7–90 (mean = 34.2; standard deviation=24.3, Table 1). The mean BSI of ramose colonies was significantly higher than that of encrusting colonies (t-Test, P = 0.002, Fig. 4b, 5b).

To test whether endozonal characters would influence the BSI results, three hypothetical ramose zoaria of 5mm in diameter but with different exozone thicknesses (Fig. 6a-c) were analysed. In these, ZWT is 0.5mm and MZD is 1mm, but EW varies from 0.5mm (Fig. 6a), 1mm (Fig. 6b) or 2mm (Fig. 6c). BSI for these zoaria is 25, 50 and 100 respectively. If Endozone Diameter (ED) is added to the formula (i.e., BSI = ((EW*ZWT)/(MZD*ED))*100) the BSI values are 6.25, 16.7 and 100. If Axial Ratio (AR) is added to the original formula (i.e., BSI = ((EW*ZWT)/(MZD*AR))*100) the values compute as 6.25, 33.3 and 200. In both cases, addition of endozonal characters does not alter the relative ranking of BSI, and given, as is outlined above, the difficulties of obtaining such data from these parameters, the BSI based on MZD, ET and IWT is sufficiently robust. If exozone thickness (EW) remains constant but endozone diameter decreases, i.e. overall branch diameter decreases (Fig. 6d-f), there is no change in BSI using the formula proposed here.

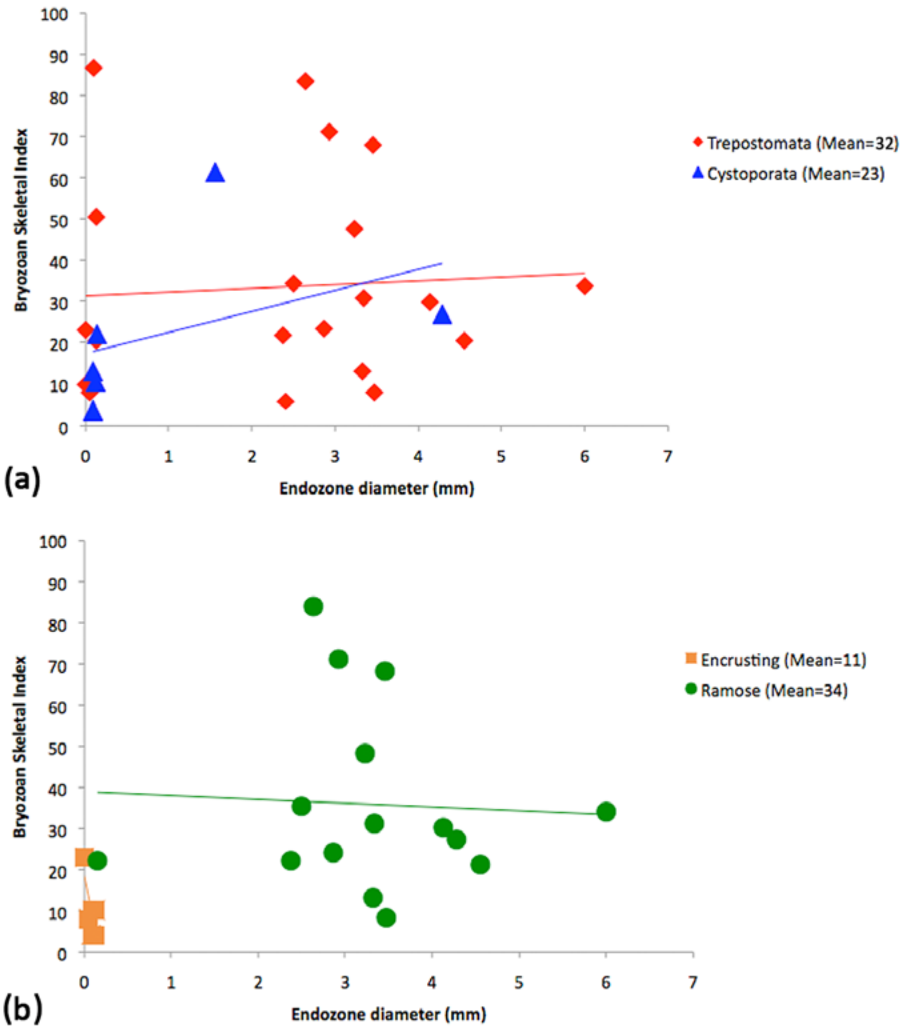

Figure 5. Plots of BSI against endozone diameter (in mm) for (a) cystoporates and trepostomes and (b) encrusting and ramose colonies.

DISCUSSION

BSI is highest in ramose trepostomes rather than ramose cystoporates or encrusing trepostomes as they have proportionally more exozone in branches and thus a lower axial ratio than do cystoporates. The differences in BSI between ramose and encrusting bryozoans are manifested in the formers' need for the skeleton to provide enough strength to allow for erect growth, and to maintain strength in water currents (Key 1991). Encrusters simply require skeleton to separate and isolate autozooecial chambers for the filter feeding lophophores; most of the strength of these colonies is provided by the foundation substrate (shell, cobble, hardground). This is also true of dome-shaped colonies such as *Diplotrypa* in which the exozonal walls are lightly calcified (Mänill 1961; Boardman and Utgaard 1966; Wyse Jackson and Key 2007) or in the turbinate *Dianulites* where the endozone and exozone cannot be distinguished on the basis of wall thickness (Taylor and Wilson 1999).

Though this study focuses on skeletal volume, it has implications for computation and assessment of colony strength (Key 1991), the biomechanics of space filling (Key *et al.* 2001), and resistance to bioerosion (Wyse Jackson and Key 2007, 2019).

The findings of this study suggest that there is merit in the adoption of the BSI in future examination of stenolaemate bryozoans, as the data generated may throw light on questions of palaeoecology, biogeochemistry, biomechanics, and biotic interactions:

(1) The volume of skeletal material in bryozoans may be related to depth, although this hypothesis remains untested for specific taxa from known different palaeo-bathymetric regimes. Branch diameter in cyclostome bryozoans has been shown to increase in cyclostome with depth (Taylor *et al.* 2007), and Figuerola *et al.* (2015) demonstrated depth-related differences in the levels of skeletal Mg-calcite in modern Antarctic bryozoans, but does the BSI vary with depth? Similarly, colony morphology

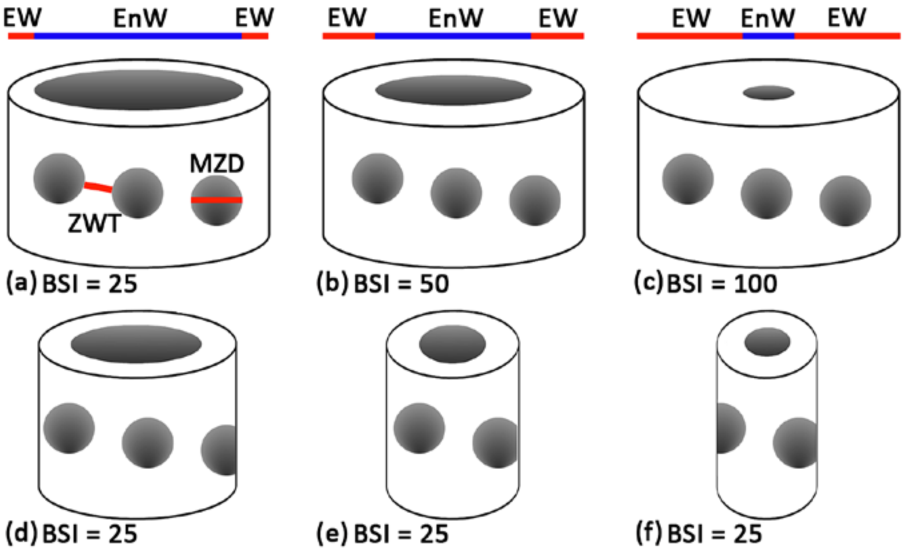

Figure 6. Stylised ramose trepostome bryozoans with (a-c) exozone of different widths (EW), (a) = 0.5mm, (b) = 1mm, (c) = 2mm in branches of 5mm diameter; (d-f) constant exozone width 0.5mm in branches of different diameter (d) = 3mm, (e) = 2mm, (f) = 1.5mm. In each colony, MZD is 1.0mm, and ZWT is 0.5mm. Abbreviation: EW: Exozone width; EnW: Endozone width; MZD: maximum autozooecial apertural diameter; ZWT: zooecial wall thickness between adjacent autozooecial apertures.

in stromatolites (Andres and Reid 2006; Jahnert and Collins 2012) varies with depth, and the ability or otherwise to lay down skeleton in bryozoans may be reflected in observable differences in zoarial or zooecial morphology.

(2) Some taxa have shown considerable plasticity in zoarial form in response to changes in environmental conditions through a small stratigraphical interval or even within reefal systems of tens of metres high. *Leioclema* a Mississippian reef of North Wales formed ramose colonies in the deepest basal facies, unilaminar sheets and bifoliate zoaria in the mid-depth facies and unilaminar sheets in the upper shallowest water zone (Wyse Jackson *et al.* 1991). While initial observations on this material suggest that BSI is similar in all zoarial forms, this needs further quantification and confirmation. Similarly, Hageman and Sawyer (2006) in a study of *Leioclema punctatum* from the Mississippian, recorded that exozone thickness was approximately the same in all specimens examined. It would be interesting to determine if there was any discernible variation in exozonal thickness between the encrusting portions of zoaria as against the erect ramose branches which subsequently developed from the bases. If so, then BSI may be able to indicate subtle changes in environmental conditions.

(3) The ability of modern bryozoans to build the hard parts of their colonies is also linked to the chemistry and levels of acidification of the oceanic waters in which they live (Smith 2009, 2014; Lombardi *et al.* 2015 and references therein). This leads to two questions: could BSI be utilised as a proxy for past oceanic chemistry or acidification, or does ocean acidification effect BSI in live bryozoan colonies or only after death through the taphonomic process?

Taylor and Kuklinski (2011) used two proxies (diameter of branches and exozonal wall thickness) in a test for hypercalcification. They concluded that these proxies either didn't demonstrate hypercalcification in the Ordovician calcite sea, or that trepostome stenolaemates didn't become hypercalclified at all. However, use of branch diameter as a proxy in this regard may be problematic as it can be altered taphonomically which results in branch flattening and loss of endozonal interiors. BSI might be a more accurate proxy for the presence or otherwise of calcite seas as it can be applied to crushed specimens.

(4) Implications of strength from skeleton. The biomechanical architecture of bryozoan colonies is one element determining strength. Cheetham and Thomsen (1981) concluded that skeletal ultrastructure and mineralogy were not demonstrable contributors to strength of colonies and their breakage under energy regimes but that the overall design of branches was more important. In ramose trepostomes, there is a positive relationship between autozooecial wall thickness and exozone width with branch strength, (Key 1991), and this study has implications for the biomechanics of space filling (Key *et al.* 2001). Quantification of the skeletal contribution via the BSI to bryozoan zoaria can add quantifiable measures for strength and the behaviour of bryozoans under different hydrodynamic regimes.

(5) It would be interesting to determine if there is a correlation between BSI and gross colony size.

(6) A high BSI may affect the ability of epibionts to penetrate zoaria and so become endoskeletozoans, and the susceptibility of these zoaria to bioerosion may thus be lessened (see Wyse Jackson and Key, 2019). This would be particularly true if epibionts attempted boring transversely across the walls, or if the diameter of the borer was greater than the autozooecial apertural diameter (MZD) where it attempted to penetrate perpendicular to the zoarial surface. Conversely, thin-walled zoaria may be more easily bored, but would have a high breakage potential and so may not be favoured by endoskeletozoans. This hypothesis will be investigated in a future study that will document BSI for Ordovician to Triassic stenolaemates from various palaeogeographic areas and draw on data on the geological record and distribution of bio-eroding organisms. Assembly of this geologically wider database may also yield evolutionary patterns of skeletal development in bryozoans.

Application of the BSI in future studies drawing on data derived from earlier literature as well as from measurements taken by the current authors, will test further potential limitations of the measure such as, what are the effects of exilazooecia, mesozooecia, diaphragms and maculae on results, and is zoarial plasticity in a single taxon reflected in a variance of BSI and in the incidence of boring?

CONCLUSION

The Bryozoan Skeletal Index (BSI) is established to provide a measure of the degree of skeletal material or calcification in stenolaemate bryozoans and is formulated from three frequently measured and thus readily available morphological characters. A study of two faunas from the Cincinnatian (Upper Ordovician) of North America has shown that the differences in BSI values between encrusting and ramose taxa is significant while that between trepostome and cystoporate taxa is not. The use of the BSI may have potential as a proxy for zoarial strength, size, and endoskeletozoan infestation as well as for investigating patterns of calcification and biomineralisation throughout the geological record of stenolaemate bryozoans.

ACKNOWLEDGMENTS

We are grateful to Susanna Wyse Jackson who kindly drafted Figure 6, and to Caroline Buttler for her insightful review.

REFERENCES

ANDRES, M.S. AND REID, R.P. 2006. Growth morphologies of modern marine stromatolites: a case study from Highborne Cay, Bahamas. *Sedimentary Geology* **185**, 319–328.

BAIRD, G.C., BRETT, C.E. AND FREY, R.W. 1989. “Hitchhiking” epizoans on orthoconic nautiloids: preliminary review of the evidence and its implications. *Senckenbergiana lethaea* **69**, 439–465.

BOARDMAN, R.S. 1960. Trepostomatous Bryozoa of the Hamilton Group of New York State. *United States Geological Survey Professional Paper* **340**, 1–87.

BOARDMAN, R.S. 1984. Origin of the post-Triassic Stenolaemata (Bryozoa): a taxonomic oversight. *Journal of Paleontology* **58**, 19–39.

BOARDMAN, R.S. 2001. The growth and function of skeletal diaphragms in the colony life of Lower Paleozoic Trepostomata (Bryozoa). *Journal of Paleontology* **75**, 225–240.

BOARDMAN, R.S. AND BUTTLER, C.J. 2005. Zooids and Extrazooidal Skeleton in the Order Trepostomata (Bryozoa). *Journal of Paleontology* **79**, 1088–1104.

BOARDMAN, R.S. AND UTGAARD, J. 1966. A revision of the Ordovician bryozoan genera *Monticulipora*, *Peronopora*, *Heterotrypa*, and *Dekayia*. *Journal of Paleontology* **40**, 1082–1108.

BROWN, G.D., JR. AND DALY, E.J. 1985. Trepostome Bryozoa from the Dillsboro Formation (Cincinnatian Series) of southeastern Indiana. *Geological Survey of Indiana, Special Report* **33**, 1–95.

BUTTLER, C.J. AND WILSON, M.A. 2018. Paleoecology of an Upper Ordovician sunmarine cave-deweeling bryozoan fauna and its exposed equivalents in northern Kentucky, USA. *Journal of Paleontology* **92**, 568–576.

CHEETHAM, A.H. 1986. Branching, biomechanics and bryozoan evolution. *Proceedings of the Royal Society of London, Series B, Biological Sciences* **228**, 151–171.

CHEETHAM, A.H. AND HAYEK, L.-A.C. 1983. Geometric consequences of branching growth in adeoniform Bryozoa. *Paleobiology* **9**, 240–260.

CHEETHAM, A.H. AND THOMSEN, E. 1981. Functional morphology of arborescent animals: strength and design of cheilostome bryozoan skeletons. *Paleobiology* **7**, 355–383.

COHEN, K.M., FINNEY, S.C., GIBBARD, P.L. AND FAN, J.-X. 2013. The ICS International Chronostratigraphic Chart. *Episodes* **36**, 199–204.

CUFFEY, R.J. AND FINE, R.L. 2005. The largest known fossil bryozoan reassembled from near Cincinnati. *Ohio Geology* **2005**(1), 1, 3–4.

CUFFEY, R.J. AND FINE, R.L. 2006. Reassembled trepostomes and the search for the largest bryozoan colonies. *International Bryozoology Association Bulletin* **2**(1), 13–15.

ERICKSON, J.M. AND BOUCHARD, T.D. 2003. Description and interpretation of *Sanctum laurentiensis*, new ichnogenus and ichnospecies, a domichnium mined into Late Ordovician (Cincinnatian) ramose bryozoan colonies. *Journal of Paleontology* **77**, 1002–1010.

ERNST, A. 2019. Fossil record and evolution of Bryozoa. In: A. Schmidt-Rhaesa (ed.), *Handbook of Zoology Online*. Berlin, De Gruyter.

ERNST, A. AND CARRERA, M. 2012. Upper Ordovician (Sandbian) bryozoan fauna from Argentine Precordillera. *Journal of Paleontology* **86**, 721–752.

FIGUEROLA, B., KUKLINSKI, P. AND TAYLOR, P.D. 2015. Depth patterns in Antarctic bryozoan skeletal

Mg-calcite: can they provide an analogue for future environmental changes? *Marine Ecology Progress Series* **540**, 109–120.

HAGEMAN, S.J. AND SAWYER, J.A. 2006. Phenotypic variation in the bryozoan *Leioclema punctatum* (Hall, 1858) from the Mississippian ephemeral host microcommunities. *Journal of Paleontology* **80**, 1047–1057.

HAQ, B.U. 2007. *The Geological Time Scale*, 6th revised edition. Amsterdam, Elsevier.

JACKSON, J.B.C. 1979. Morphological strategies of sessile animals. In: G.P. Larwood and B.R. Rosen (eds), *Biology and Systematics of Colonial Organisms.* London, Academic Press, pp. 499–555.

JAHNERT, R.J. AND COLLINS, L.B. 2012. Characteristics, distribution and morphogenesis of subtidal microbial systems in Shark Bay, Australia. *Marine Geology* **303–306**, 115–136.

KARKLINS, O.L. 1984. Trepostome and cystoporate bryozoans from the Lexington Limestone and the Clay Ferry Formation (Middle to Upper Ordovician) of Kentucky. *United States Geological Survey Professional Paper* **1066-I**, 1–105.

KEY, M.M., JR. 1990. Intracolony variation in skeletal growth rates in Paleozoic ramose trepostome bryozoans. *Paleobiology* **16** (4), 483–491.

KEY, M.M., JR. 1991. How to build a ramose trepostome. In: F.P. Bigey and J.-L. d'Hondt (eds), Bryozoaires actuels et fossiles: Bryozoa living and fossil. *Bulletin de la Société des Sciences Naturelles de l'Ouest de la France. Mémoire HS* **1**, 201–207.

KEY, M.M., JR., THRANE, L. AND COLLINS, J.A. 2001. Space-filling problems in ramose trepostome bryozoans as exemplified in a giant colony from the Permian of Greenland. *Lethaia* **34**(2), 125–135.

KEY, M.M., JR., WYSE JACKSON, P.N. AND FELTON, S. 2016. Intracolony variation in zoarial morphology in reassembled fossil ramose stenolaemate bryozoans from the Upper Ordovician (Katian) of the Cincinnati Arch region, USA. *Journal of Paleontology* **90**(3), 400–412.

LOMBARDI, C., COCITO, S., GAMBI, M.C. AND TAYLOR, P.D. 2015. Morphological plasticity in a calcifying modular organism: evidence from an *in situ* transplant experiment in a natural CO_2 vent system. *Royal Society Open Science* **2**, 140413.

MA, J., BUTTLER, C.J. AND TAYLOR, P.D. 2014. Cladistic analysis of the 'trepostome' Suborder Estonioporina and the systematics of Palaeozoic bryozoans. *Studi Trentini di Scienze Naturali* **94**, 153–164.

MÄNNIL, R.M. 1961. On the morphology of the hermispherical Bryozoa of the Order Trepostomata. *Eesti NSV Teaduste Akadeemia Geoloogia Instituudi Uurimused* **6**, 113–140.

POWERS, C.M. AND PACHUT, J.F. 2008. Diversity and distribution of Triassic bryozoans in the aftermath of the end-Permian mass extinction. *Journal of Paleontology* **82**, 362–371.

SMITH, A.M. 2009. Bryozoans as southern sentinels for ocean acidification: a major role for a minor phylum. *Marine and Freshwater Research* **60**, 475–482.

SMITH, A.M. 2014. Growth and calcification of marine bryozoans in a changing ocean. *Biological Bulletin* **226**, 203–210.

SMITH, A.M. 2018. Bryozoans and ocean acidification. In: P.L. Cook, P.E. Bock, D.P. Gordon and H.J. Weaver (eds), *Australian Bryozoa Volume 1: Biology, Ecology and Natural History*. Clayton South, Victoria, CSIRO publishing, pp. 139–144.

TAYLOR, P.D. AND KUKLINSKI, P. 2011. Seawater chemistry and biomineralisation: did trepostome bryozoans become hypercalcified in the 'calcite sea' of the Ordovician? *Palaeobiodiversity and Palaeoenvironments* **91**, 185–195.

TAYLOR, P.D., KUKLINSKI, P. AND GORDON, D.P. 2007. Branch diameter and depositional depth in cyclostome bryozoans: testing a potential paleobathymetric tool. *Palaios* **22**, 220–224.

TAYLOR, P.D. LOMBARDI, C. AND COCITO, S. 2015. Biomineralization in bryozoans: present, past and future. *Biological Reviews* **90**, 1118–1150.

TAYLOR, P.D. AND WILSON, M.A. 1999. *Dianulites* Eichwald, 1829: an unusual Ordovician bryozoan with a high-Magnesium Calcite skeleton. *Journal of Paleontology* **73**, 38–48.

VAN HINSBERGEN, D.J.J., DE GROOT, L.V., VAN SCHAIK, S.J., SPAKMAN, W., BIJL, P.K., SLUIJS, A., LANGEREIS, C.G. AND BRINKHUIS, H. 2015. A Paleolatitude Calculator for Paleoclimate Studies. *PLoS ONE* **10**(6), 1–21 [Model version 2.1 online: www.paleolatitude.org]

WILSON, M.A., BUTTLER, C.J. AND TAYLOR, P.D. 2019. Bryozoans as taphonomic engineers, with examples from the Upper Ordovician (Katian) of Midwestern North America. *Lethaia* **52**, 403–409.

WYSE JACKSON, P.N., BANCROFT, A.J. AND SOMERVILLE, A.J. 1991. Bryozoan zonation in a trepostome-dominated buildup from the Lower Carboniferous of North Wales. In: F.P. Bigey and J.-L. d'Hondt (eds), Bryozoaires actuels et fossiles: Bryozoa living and fossil. *Bulletin de la Société des Sciences Naturelles de l'Ouest de la France. Mémoire HS* **1**, 551–559.

WYSE JACKSON, P.N. AND KEY, M.M., JR. 2007. Borings in trepostome bryozoans from the Ordovician of Estonia: two ichnogenera produced by single maker, a case of host morphology control. *Lethaia* **40**, 237–252.

WYSE JACKSON, P.N. AND KEY, M.M., JR. 2019. Epizoan and endoskeletozoan distribution across reassembled ramose stenolaemate bryozoan zoaria from the Upper Ordovician (Katian) of the Cincinnati Arch region, USA. *Memoirs of the Association of Australasian Palaeontologists* **52**, 169–178.

WYSE JACKSON, P.N., KEY, M.M., JR. AND COAKLEY, S.P. 2014. Epizoozoan trepostome bryozoans on nautiloids from the Upper Ordovician (Katian) of the Cincinnati Arch Region, U.S.A.: an assessment of growth, form and water flow dynamics. *Journal of Paleontology* **88**(3), 475–487.

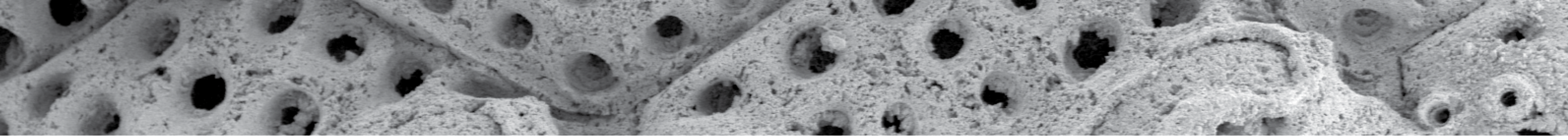

18TH
INTERNATIONAL
BRYOZOOLOGY
ASSOCIATION
CONFERENCE

BRYOZOAN STUDIES 2019

Edited by Patrick Wyse Jackson & Kamil Zágoršek

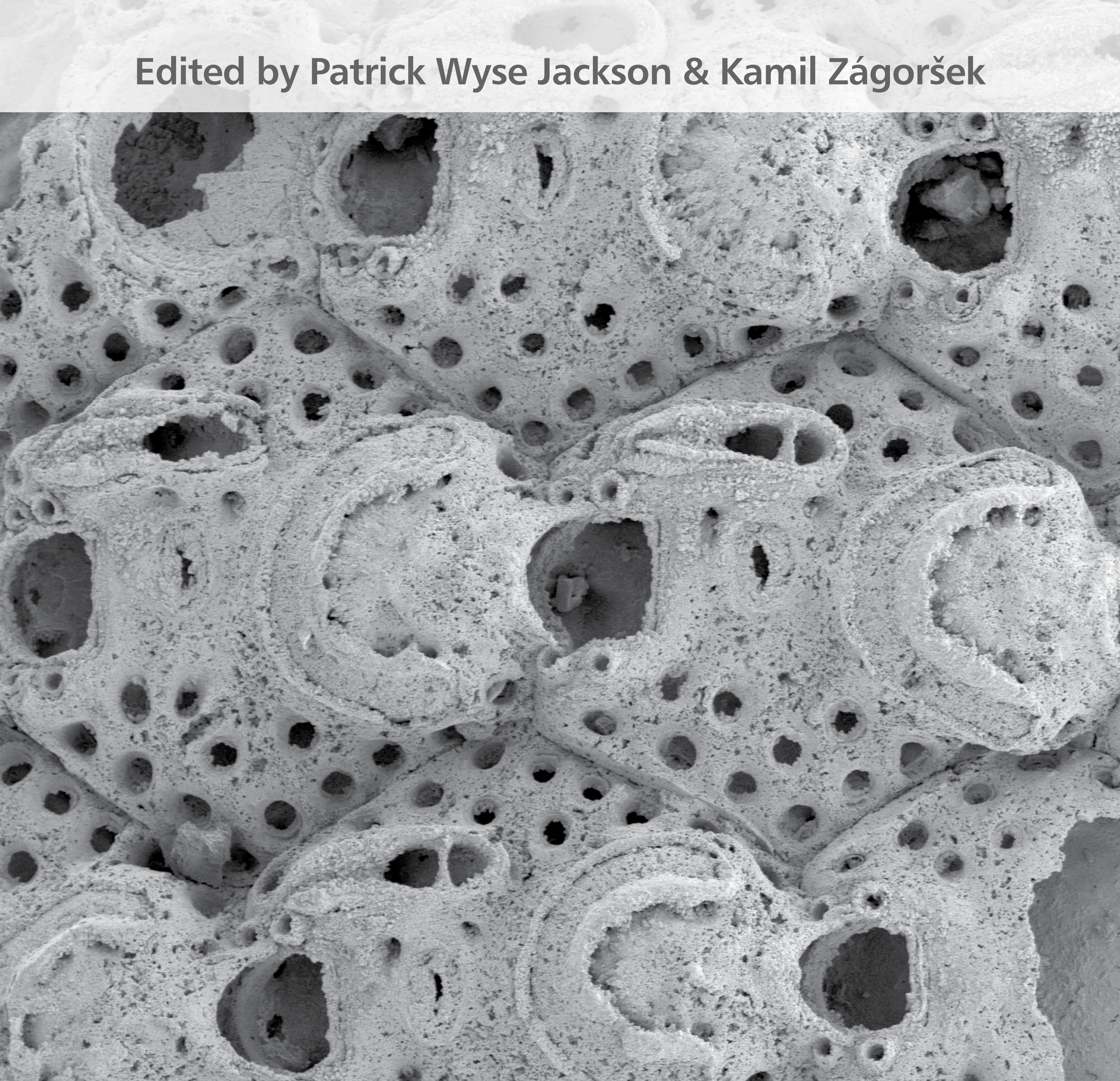

18TH
INTERNATIONAL
BRYOZOOLOGY
ASSOCIATION
CONFERENCE

1919
CZECH GEOLOGICAL SURVEY

IBA International Bryozoology Association

Cover illustration: *Calloporina decorata* (Reuss, 1847)
from section Sedlec (South Moravia – Czech Republic)

Bryozoan studies 2019 – Proceedings of the eighteenth International Bryozoology
Association Conference Liberec – Czech Republic, 16th to 21st June 2019

Editors: Patrick Wyse Jackson & Kamil Zágoršek
Graphic design: Eva Šedinová
Printing: Reprographic Centre of the Czech Geological Survey
Published by the Czech Geological Survey, Prague 2020

ISBN 978-80-70759-70-7